JOURNAL OF GEOPHYSICAL RESEARCH, VOL. 112, A10101, doi:10.1029/2006JA012117, 2007

Long-term changes in the cosmic ray intensity at Earth, 1428–2005

K. G. McCracken[1] and J. Beer[2]

Received 12 October 2006; revised 9 June 2007; accepted 27 June 2007; published 5 October 2007.

[1] The instrumental cosmic ray data recorded in the interval 1933–1965 by S. E. Forbush and H. V. Neher and cosmogenic ^{10}Be data are merged with the neutron monitor data since 1951 to study the long- and short-term variations in the galactic cosmic radiation intensity for the interval 1428–2005. It is shown that the ionization chamber data published by S. E. Forbush were deliberately detrended to remove long-term changes. The high-altitude ionization chambers used by H. V. Neher during this interval were well calibrated and their data exhibit a substantial decrease between 1933 and 1954 that is consistent with the long-term trends in the cosmogenic ^{10}Be data. Using the specific yield functions appropriate to neutron monitors, ionization chambers, and ^{10}Be, the nonlinear relationships between these data types are determined. It is shown that the nonlinearities are large and will introduce serious errors if ignored. An intercalibrated record (the ''pseudo-Climax neutron monitor record'') is developed for the interval 1428–2005. It is used to study several features of the long-term periodicities in the cosmic radiation, after discussion of residual effects due to meteorological effects, and the production of ^{10}Be by solar cosmic rays. It is shown that (1) the average intensity in the neutron monitor energy range for the interval 1954–1996 is ~16% less than the average for the period 1428–1944 and that it shows a consistency and depth of modulation that had not occurred in the previous 580 years. (2) The residual cosmic ray modulation was low throughout the Gleissberg cycle 1540–1645, considerably higher for the next two Gleissberg Cycles, and highest of all since 1944. (3) The cosmogenic data imply that solar activity was anomalously low throughout the whole interval 1428–1715, the amplitude of the solar activity during the Gleissberg cycle 1540–1645 being ~50% of that during the following two Gleissberg cycles and ~25% of that in the post-1954 era. (4) It is proposed that the steadily increasing cosmic ray modulation since 1428 constitutes a quarter cycle of the previously identified 2300 year periodicity in the cosmogenic data. (5) The cosmic ray intensity decreased in two steps between 1889 and 1901 and 1944 and 1954, in broad agreement with the two-step increase in heliomagnetic field strength determined by Schrijver et al. (2002). It is proposed that the ''pseudo-Climax neutron record'' will be of benefit in the normalization of other cosmogenic records to the neutron monitor record starting in 1951.

Citation: McCracken, K. G., and J. Beer (2007), Long-term changes in the cosmic ray intensity at Earth, 1428–2005, *J. Geophys. Res.*, *112*, A10101, doi:10.1029/2006JA012117.

1. Introduction

[2] The sunspot, auroral, and geomagnetic records all exhibit substantial long-term variations. All three exhibit active periods similar to that observed during the period 1950–2000 AD and quiet periods such as the three ''Grand Minima,'' the Spoerer (1420–1540), Maunder (1645–1715), and Dalton (1800–1830) Minima. Unlike the sunspot and geophysical data, there is no continuous cosmic ray record from the past centuries to the present. In this paper, four separate cosmic ray records are intercalibrated to allow us to study the long-term changes in the cosmic ray intensity between 1428 and 2005. In particular, this allows us to study the long-term cosmic ray changes since 1900 and to compare the intensities observed in the ''space age'' 1965–2005 with those observed over the past 500 years.

[3] The neutron monitor record started in 1951 and is the most commonly used measure of the cosmic ray intensity at Earth. Since 1951, the neutron counting rates have returned to within ~2% of the same value in each of the sunspot minima 1954, 1965, 1976, 1987, and 1997, and there is little indication of a long-term change in the residual modulation observed at sunspot minimum over these four solar cycles. *Beer* [2000] has shown that the sequestration of ^{10}Be in polar ice constitutes a natural neutron monitor, whose record extends >10,000 years into the past. By way

[1]Institute for Physical Science and Technology, University of Maryland, College Park, Maryland, USA.
[2]Swiss Federal Institute of Aquatic Science and Technology (EAWAG), Duebendorf, Switzerland.

0148-0227/07/2006JA012117$09.00

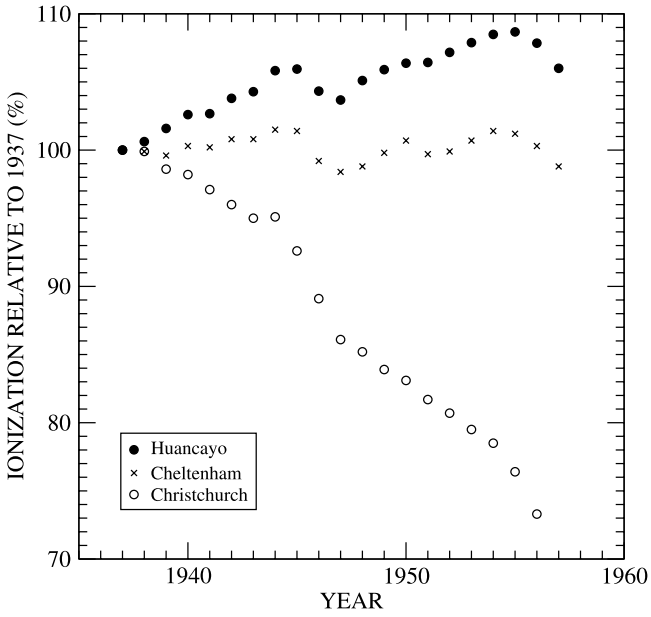

Figure 1. The annual average ionization rates observed by the Huancayo, Cheltenham, and Christchurch ionization chambers between 1937 and 1957 prior to the corrections that were made by *Forbush* [1954, 1958] to remove long-term drifts. The data are normalized to 100% for 1937.

of contrast with the neutron monitor, the concentration of cosmogenic ^{10}Be indicates that there have been long-term changes in the cosmic ray intensity over timescales of ~100 years and that the present epoch since 1950 exhibits one of the lowest intensities observed in the past 1000 years [*McCracken et al.*, 2004a]. In particular, the ^{10}Be concentration measured at Dye 3 (Greenland) for the 11-year period centered on 1889 was $\sim 1.3 \times 10^4$ atoms/g, i.e., 53% above the concentration of $\sim 0.85 \times 10^4$ atoms/g for the sunspot minima of 1965 and 1976. That is, the ^{10}Be data show that there was a substantial decline in cosmic ray intensity in the several decades prior to the commencement of the neutron monitor record in 1951. Further support is given by the ^{14}C data from tree rings, after correction for the increasing level of anthropogenic CO_2 [*Muscheler et al.*, 2007].

[4] S. E. Forbush published ground-level ionization chamber records for the period 1936–1968, and these were a mainstay of cosmic ray research for 3 decades. Inevitably, these data were used to extrapolate the neutron data back from the 1950s, to 1936 (*Rao* [1972], and then used by *O'Brien* [1979] and others), leading to the conclusion that there was no long-term change in the cosmic radiation intensity at Earth between 1936 and 1952. This paper points out that Forbush had detrended his data and had deliberately removed all long-term trends other than the 11-year variation. Consequently, the Forbush data by themselves provide no information about the long-term trends in the cosmic ray intensity at Earth. However, between 1933 and 1969, H. V. Neher and his coworkers made an independent series of well-calibrated ionization chamber measurements at high altitudes and *Neher* [1971] concluded that there had been a substantial decrease in cosmic ray intensity over this 36-year period. This result has been disregarded due to lack of independent confirmation (the ability to measure ^{10}Be with high temporal resolution was not developed until 1980).

[5] The cosmogenic ^{10}Be, the neutron monitor, and the ionization chambers are sensitive to different regions of the comic ray spectrum. The cosmic ray modulation process is strongly energy dependent, and as a consequence there are nonlinear relationships between the fluctuations observed in those data [*Mursula et al.*, 2003; *McCracken*, 2004]. An important goal of this paper is to calculate those nonlinear relationships and use them to combine the data from the Climax neutron monitor, the ionization chambers, and the ^{10}Be record, to yield an intercalibrated record that can then be used to study the long-term changes in the cosmic ray intensity.

[6] In combining these data, it was necessary to allow for the secular changes in the strength of the geomagnetic field and the changing location of the geomagnetic pole. Both introduce long-term changes into the geomagnetic cutoff rigidities worldwide. The ^{10}Be record was corrected to the present epoch as discussed by *McCracken et al.* [2004a] prior to combination with the other data. The Climax geomagnetic cutoff has changed substantially with time [*Shea and Smart*, 2003]; in this paper the several data sets have been combined to correspond to a constant cutoff equal to the present day value of 3.15 GV. We call this the pseudo-Climax time series.

[7] The paper proceeds as follows: (1) it summarizes the characteristics of the Forbush and Neher observations that will be used with the neutron monitor and ^{10}Be data; (2) section 2 presents the specific yield functions for ^{10}Be, neutron monitors at two atmospheric depths and an ionization chamber at an atmospheric depth of 100g/cm^2. (3) Section 3 then investigates the nonlinearity of all the responses and computes nonlinear intercomparison curves; (4) section 4 uses the several data types to estimate the neutron monitor variations for the whole of the instrumental era 1933–2005. In this, the well-calibrated Neher observations provide the long-term changes that Forbush removed from his data (1936–1957). Using a nonlinear intercalibration curve, the ^{10}Be data (1428–1933) are normalized to the present day Climax neutron monitor. Together, these data are used to study the nature of the 11-year and longer-term changes in the cosmic ray intensity since the middle ages. The companion paper then uses the inversion technique of *Caballero-Lopez et al.* [2004] to investigate the strength of the heliomagnetic field near Earth between 1428 and 2000 AD, with particular emphasis on the period 1889–1965.

2. Long-Term Stability of the Carnegie Ionization Chamber Record

[8] A worldwide network of five ionization chambers was established by the Carnegie Institution in 1936 [*Compton et al.*, 1934; *Lange and Forbush*, 1948], that led to the discovery of the majority of the known time variations in the cosmic ray intensity. It should be noted, however, that Forbush never made any statements regarding the long-term changes in the cosmic ray intensity other than those regarding the 11-year variation that was clearly in antiphase with the sunspot cycle [*Forbush*, 1954]. Examination of

Figure 1 shows why. It presents the original annual averages of the ionization currents, after correction for changes in the atmospheric pressure and "bursts" (nuclear reactions in the walls of the chamber). Comparing the data between 1937 and 1952, we note that (1) the Christchurch ionization current decreased by ~30%, (2) Cheltenham was essentially invariant, and (3) Huancayo increased by 6%. Godhavn (Greenland; not shown) decreased by 3.7%. The 11-year variation in all four instruments was ~3.5%, indicating similar sensitivities to changes in the cosmic ray intensity. It is therefore clear that there was severe disagreement between all four instruments regarding any longer-term changes in the cosmic ray intensity.

[9] This disagreement was not unexpected. The Compton-Bennett ionization chamber, while a marked improvement on its predecessors, was nevertheless subject to long-term drifts. It had been designed to measure time-dependent changes of ~0.3% over several years, and for this reason it was a difference instrument. The ionization current from the 19 liter main chamber was balanced by a current of opposite sign from the "compensation (or balance) chamber" containing a radioactive source (uranium) inside the main chamber. This greatly reduced the chambers' sensitivity to environmental effects and to a number of instrumental effects (e.g., changing voltages, changing gas temperature and pressure in the chamber) yielding good stability on the short to medium term (~5 years). The position of the uranium source was adjustable to allow the balance to be adjusted to keep the instrument "on scale." Over time, this was done on all chambers other than the one at Cheltenham. The Uranium source also contributed ~15% of the ionization current in the main chamber [*Compton et al.*, 1934], the amount being determined by the position of the source in the balance chamber. This resulted in poorly known changes in the current in the main chamber due to the changes in the source position. Forbush clearly recognized [*Forbush*, 1954, 1958] that the decay of radioactive contamination in either chamber, together with the variable contribution from the uranium source, would result in long-term changes of either sign in the recorded data. The size and stability of such background effects could be established by operating the ionization chambers in a moderately deep mine or tunnel, as was done initially as part of the construction and commissioning of one chamber [*Compton et al.*, 1934]. There is no record, however, that this was done again for any of the chambers to examine the long-term effects. Without any other independent means to calibrate the long-term stability of the instruments, Forbush was restricted to investigating periodic or episodic variations that could be validated by correlation with other phenomena.

[10] *Forbush* [1954] therefore stated "(the data were) corrected for these linear (long-term) changes, which are assumed to arise from decay of radioactive contamination in the main chamber or in the balance chamber." The long-term invariance observed for Cheltenham was assumed to indicate the absence of instrumental drifts for that instrument. Forbush therefore superimposed linear trends on the Christchurch and Godhavn data and an exponential trend on the Huancayo data to yield the same invariance between 1937 and 1957 that was observed for Cheltenham [*Forbush*, 1958]. (In modern parlance, Forbush detrended the data.) Note that he never claimed that this had removed the long-term instrumental drifts from the data. His intention was to permit the study of cyclic and episodic events in the four data sets, and to this end he applied a mathematical adjustment so that these several temporal changes would be superimposed upon a constant baseline of unknown origin. At that time, there was no evidence available to determine whether the invariance of the Cheltenham data was due to a long-term instrumental drift compensating for a long-term change in the cosmic ray intensity.

[11] Without this background, and ignoring the correction procedures detailed by *Forbush* [1954, 1958], others have taken the published Forbush data at face value and used them to investigate the long-term changes in the cosmic ray intensity between 1936 and 1957 and to normalize the cosmogenic ^{14}C record to the neutron monitor record, 1951–date. It is important to note the following:

[12] 1. The similarity in the long-term changes in the four ionization chamber data sets as published is a direct consequence of the ad hoc corrections for instrumental drift applied by Forbush.

[13] 2. The apparent invariance between 1937and 1952 observed at Cheltenham, and then imposed on the other data sets, may be due to a fortuitous compensation of a long-term change in the cosmic ray intensity, by a long-term instrumental drift of the opposite sign, similar to those observed in the other three ionization chambers.

[14] 3. An external, independent method must be used to provide the long-term variation in the cosmic ray data, which will then allow the effects of the instrumental drifts to be removed from the Cheltenham and other ionization chamber data.

3. Neher High-Altitude Ionization Chambers

[15] Starting in 1933, H. V. Neher and his coworkers developed and flew unshielded ionization chambers to atmospheric depths of 15 g/cm^2 and less [*Neher*, 1953, 1967, 1971, and references therein]. The instrumental requirements were greatly different from those of the Compton Bennett chambers, and accurate long-term calibration was an inherent feature of his measurements. This was primarily due to the ionization currents at high altitudes being a factor of 100–400 above those at sea level, and as a consequence, the effects of radioactive contamination on the high-altitude observations were very small. In addition, a direct calibration of the sensitivity of each chamber was made prior to flight as outlined below. The large dynamic range and the nature of the measurements meant that a compensation chamber was not required, as in the case of the Compton Bennett chambers, and the uncertainty of positive and negative drifts was avoided.

[16] Neher maintained a very careful calibration procedure described by *Neher and Anderson* [1964] and *Neher* [1971, and references therein] that can be traced back to a reference ionization chamber constructed by *Millikan and Cameron* [1928]. Three versions of the ionization chamber were used: (1) a photographic recording version used between 1936 and 1946, (2) the first version of an instrument that telemetered the results to Earth used between 1951 and 1956, and (3) an improved version of the ionization chamber used between 1957 and 1969. *Neher* [1971] discusses the correction for the small change in the

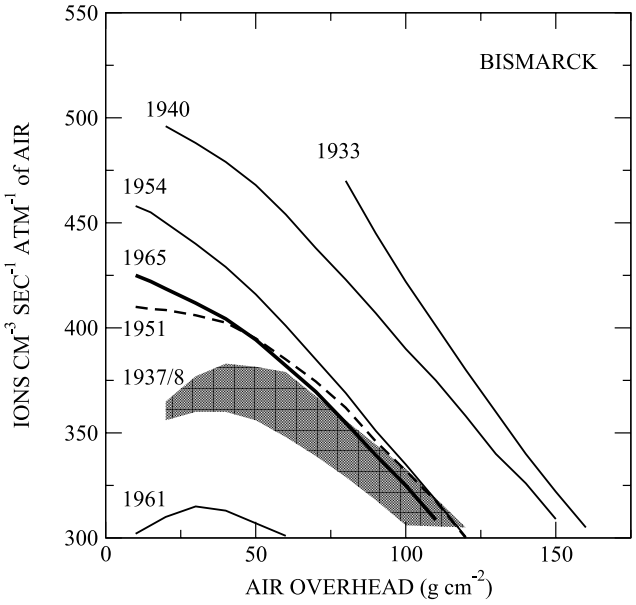

Figure 2. The observed cosmic ray ionization rate versus atmospheric depth during the interval 1940–1965 at Bismarck, South Dakota, and the data from the "Century of Progress" balloon flight in 1933. The majority of the curves are averages over several flights. The grey band labeled 1937/1938 represents 18 different balloon flights during that interval. Appendix A discusses experimental factors relating to the curve for 1933. The different curve shapes above 75g cm^{-2} are a consequence of the low intensities of <50 MeV/nucleon cosmic rays near sunspot maximum (e.g., 1961, 1937–1938) compared to high intensities near sunspot minimum (e.g., 1954, 1965).

ionization chamber wall thickness between versions 1 and 2 and analyzes the detailed intercalibrations of the three versions that occurred in 1951, 1954, 1956, and 1970. On the basis of these intercalibrations, he concluded that "if any slippage of the calibration has occurred during the past 33 years, it cannot be greater than ±1%" [*Neher*, 1971]. To eliminate interflight differences due to manufacturing and other irregularities, each chamber was calibrated prior to flight against a number of reference chambers. In the calibrations, a gamma ray source was placed at a fixed distance that yielded an ionization current similar to that observed at high altitudes. This yielded the sensitivity of each chamber relative to the long-term calibration chambers that included one used for the measurements in the 1930s. In addition, two or three chambers were sometimes flown within several hours of one another to check the reproducibility of the measurements. Instrumental and systematic errors were estimated to be ~0.5–1% [*Neher*, 1956]. Fortuitously, he frequently used Bismarck, South Dakota (geomagnetic cutoff = 1.29 GV) as a "base station" for other measurements, and this provides a set of directly comparable measurements over the period 1938–1969. Figure 2 presents a selection of the ionization curves obtained over the period 1933–1969, and it is clear that there was a strong variation with time.

[17] The neutron monitor is sensitive to galactic cosmic rays with rigidities ≥1 GV, corresponding to proton energies ≥420 MeV. Such protons can penetrate to an atmospheric depth of ~100 g/cm^2, suggesting that the ionization at this atmospheric depth might be a suitable proxy for the ground-level neutron monitor. To verify this, Figure 3 displays the correlation between the 100 g/cm^2 ionization current observed at Thule, Greenland (cutoff rigidity ≈ 0.0 GV), and the Climax neutron monitor, together with the nonlinear interdependence computed in section 5, and good agreement is evident. Other data [*Neher*, 1961] show that the 100 g/cm^2 ionization current does not change significantly for cutoff rigidities <1 GV. That is, the 100 g/cm^2 ionization current reproduces the cosmic ray "knee" near 1 GV, and the "plateau" at <1 GV, observed for the ground-level neutron monitor. On the basis of both verifications, the 100 g/cm^2 ionization current at Bismarck (henceforth represented by I(B, t)) is used throughout this paper as a nonlinear proxy for the neutron monitor counting rates prior to 1951.

[18] The year 1940 was 4 years prior to the sunspot minimum of 1944, and a substantial degree of residual 11-year modulation would have still been present (particularly so, since this was a qA < 0 solar minimum). Nevertheless, Figure 2 shows that the ionization rate for 1940 was ~15% higher than during the sunspot minimum of 1954. The band of measurements in Figure 2 for 1937–1938 is derived from four independent measurement campaigns (a total of 18 flights), and it shows that the 100 g/cm^2 ionization rate near the maximum of solar activity (sunspot

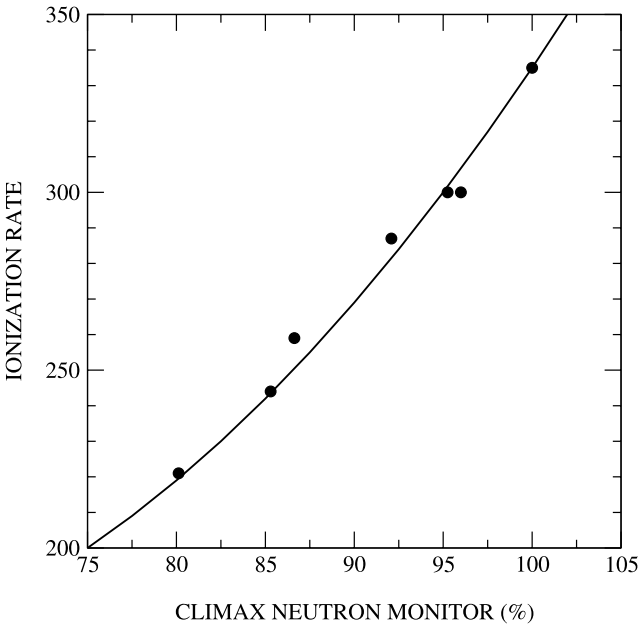

Figure 3. The correlation between the ionization rate at an atmospheric depth of 100 g/cm^2 at Thule Greenland, and the Climax neutron monitor, over the interval 1954–1965. The ionization rate is given in ion pairs/(cm^3 s atmosphere of air). The Climax data are normalized to 100% for 1954. The superimposed curve is the nonlinear interdependence between these data from Figure 5, based on the specific yield functions in Figure 4. It was scaled to pass through the observed point in the top right hand of the figure, with no adjustments for slope to fit the other data points.

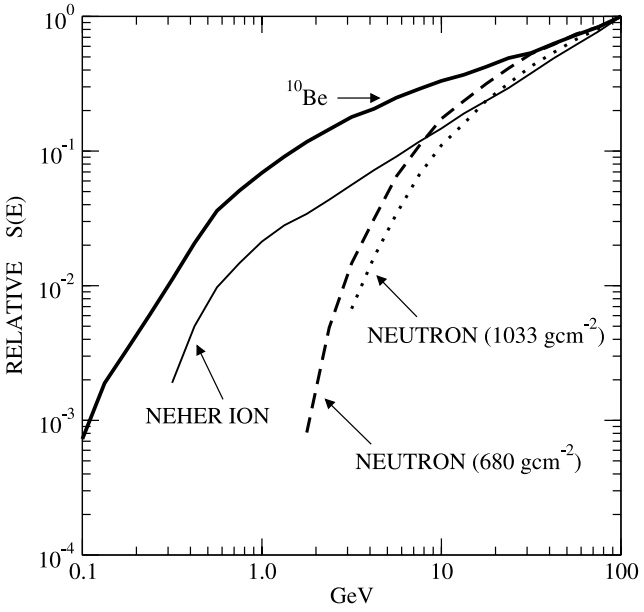

Figure 4. The specific yield functions for cosmic ray protons applicable to four different types of cosmic ray measurement. See text for further details.

number 145 in late 1937) approximated those observed during the sunspot minima of 1954 and 1965. While possibly suspect (see Appendix A), the curve for the sunspot minimum of 1933 is well above those for the minima of 1954 and 1965. All three comparisons indicate that the cosmic ray intensity was substantially higher during the 1933–1944 solar cycle than during the cycles after 1954.

[19] *McCracken et al.* [2004a] have shown that the concentration of the cosmogenic ^{10}Be stored in polar ice is well correlated between South Pole and Greenland and have concluded that those data provide a reliable indication of the long-term variations in the cosmic ray flux in the vicinity of 1–2 GeV/nucleon. Further, they concluded that the cosmic ray flux in the vicinity of Earth since ~1950 has been one of the lowest in the past 1000 years. Their Figure 1 shows that the concentration of ^{10}Be in Greenland and Antarctica exhibited a declining trend between ~1900 and ~1954. The ^{14}C data analyzed by *Muscheler et al* [2007] exhibit a similar declining trend. All three cosmogenic records provide independent support for the conclusion based upon the Neher ionization data.

4. Specific Yields and Intercalibration of Instruments

[20] The output of the kth cosmic ray detector at time t is given by

$$G_k(t) = \sum_i \int_{E_{c,k,i}}^{\infty} S_{k,i}(E).\ J_i(E,t)\ dE \qquad (1)$$

where E is the cosmic ray kinetic energy per nucleon, $J_i(E, t)$ is the cosmic ray energy spectrum in the vicinity of Earth for the ith component (protons, alphas, etc.), and $S_{k,i}(E)$ is the specific yield function for the kth detector and the ith component of the cosmic radiation. $E_{c,k,i}$ is the geomagnetic cutoff energy/nucleon for the ith component and kth detector, given by $[\{(Z/A)^2 R_c^2 + 1\}^{0.5} - 1]$, where Z and A are the charge and atomic mass of the cosmic rays and R_c is the cutoff rigidity.

[21] In the past, the specific yield functions used in equation (1) were estimated from the observed latitude dependence of neutron monitors and ionization chambers. This provided no information above 15 GeV/nucleon, and the estimates above that energy were particularly subject to uncertainty for ground-level ionization chambers. Nor did it provide the yield functions for protons and helium nuclei. The modulation and geomagnetic effects of these components are significantly different, and individual computation is particularly important for measurements where the yield functions are significant below 1 GeV/nucleon [*Webber and Higbie*, 2003; *McCracken*, 2004]. In recent years, all the specific yields considered here have been computed using Monte Carlo codes that simulate the nucleonic cascade in the atmosphere, using the best available cross sections for all energies to >100 GeV/nucleon. As such, the several specific yield functions are internally consistent and quantify the contributions of the higher-energy portion of the cosmic ray spectrum more accurately than in the past.

[22] Figure 4 displays some of the specific yield functions for cosmic ray protons for a number of cosmic ray detection systems. The IGY neutron monitor curves were obtained by combining the directional calculations for protons and alpha particles from *Clem and Dorman* [2000] with the experimental results of *Nagashima et al.* [1989]. The IGY neutron monitor curves are for sea level, and 680g/cm^2, approximating Climax, Colorado. The Neher ionization chamber curve is the curve for 100 g/cm^2 computed from the data given by *Usoskin and Kovaltsov* [2006]. The ^{10}Be curve is from *Webber and Higbie* [2003]. All the curves have been normalized at 100 GeV/nucleon to permit intercomparison. The relative sensitivities of these several data types are evident in Figure 4. It is clear that ^{10}Be and an ionization chamber at 100 g/cm^2 have significant sensitivity below 1 GeV/nucleon, while the others do not. The curve for a 680 g/cm^2 neutron monitor is systematically more sensitive to the lower energies than is a sea level neutron monitor.

[23] Equation (1) was then evaluated for protons and alpha particles using the specific yield functions such as in Figure 4, for each data type, cosmic ray species, and for eight different cosmic ray spectra, corresponding to values of the modulation potential between 0 and 1000 MV. (The modulation potential, φ, is described in the work of *Gleeson and Axford* [1968] and *McCracken et al.* [2004a].) The local interstellar spectra were those given by *Webber and Lockwood* [2001]. The Climax geomagnetic cutoff rigidity was taken to be invariant at 3.15 GV [*Shea and Smart*, 2003]. Numerical integration was used to 115 GeV/nucleon and an indefinite integral was used from 115 GeV/nucleon to infinity. Writing the computed values of $G_k(t)$ for modulation potential φ as $G_k(\varphi)$, the ratios $G_k(\varphi)/G_k(\varphi = 0)$ were computed for each data type. Each gave the ratio of the output for modulation potential φ, to that which would be observed by that instrument in the absence of any modulation. In the case of the pseudo-Climax neutron

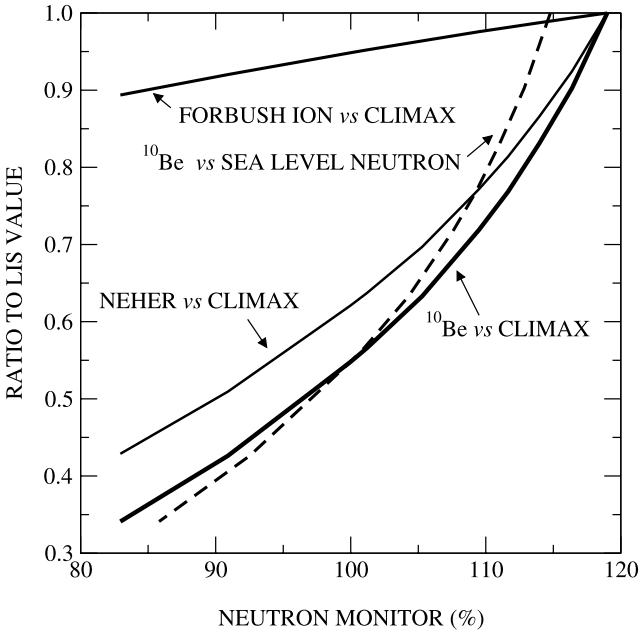

Figure 5. The computed interrelation of five different measurements of the cosmic ray intensity subject to various levels of modulation. The responses on the Y axis are the ratio between the stated type of measurement, and its value if the local interstellar spectrum (LIS) were incident on Earth (i.e., $G_k(\varphi)/G_k(\varphi = 0)$ as described in the text). The neutron monitor response on the X axis is the percentage relative to that at the sunspot minima since 1954 (i.e., 100 times the ratio $G_k(\varphi)/G_k(\varphi = 450$ GV) as discussed in the text).

output, the ratio $G_k(\varphi)/G_k(\varphi = 450$ MV) was computed as well, to indicate the ratio of the pseudo-Climax output to a value representative of the sunspot minima since 1954.

[24] The ^{10}Be is produced by high-energy spallation reactions between cosmic ray secondaries (mainly neutrons) and nitrogen and oxygen throughout the Earth's atmosphere. The production rate is largest at high altitudes at high latitudes. After a mean residence time of about 1 year, ^{10}Be is removed from the atmosphere preferentially by wet precipitation (rain and snow). The fallout in the polar caps depends on the latitudinal distribution of the production rate, the degree of atmospheric mixing and the deposition processes. For the purpose of this paper we use the M3 mixing model of *McCracken* [2004] that assumes a linearly increasing contribution from 0 to 100% between geographic latitudes of 20°and 60° and 100% for latitudes >60°. That is, equation (1) was evaluated for the ^{10}Be specific yield function in Figure 4, and the percentage change from the LIS value reduced by the factor appropriate to the M3 model.

[25] Figure 5 displays the resulting relationships between (1) ^{10}Be and the pseudo-Climax neutron monitor, and ^{10}Be and a high-latitude sea level neutron monitor; (2) the Neher 100 g/cm^2 ionization rate and Climax neutron; and (3) Climax neutron and a ground-level ionization chamber. Note that all the relationships except the last are substantially nonlinear. For example, the gradient of the ^{10}Be and pseudo-Climax neutron curve changes by a factor of 2.7 between the periods near the Maunder and Dalton minima ($0 < \varphi < 200$ MV) and the period since 1951 ($500 < \varphi < 1000$ MV). Figure 5 shows that the use of a linear regression derived from the period after 1951 would yield an estimate of 136% for $\varphi = 0$ MV, compared to 119.5% for the computed nonlinear relationship. All the interrelationships between ^{10}Be, the neutron monitors as a class, and the ionization chambers exhibit similar errors if a linear regression is used. The nonlinear interrelationships in Figure 5 are used throughout the rest of this paper.

[26] *McCracken et al* [2004a] introduced the nomenclature ^{10}Be(LIS) to represent the estimated value of the ^{10}Be concentration if the cosmic ray local interstellar spectrum (LIS) were incident on Earth (that is, the modulation potential, $\varphi = 0$ MV). The reader is referred to that paper for discussion of the concept and its estimation. For consistency, the term Cnm(LIS) will be used here to denote the estimated value of the pseudo-Climax neutron monitor counting rate if there were no cosmic ray modulation. From Figure 5, Cnm(LIS) = 119.5%.

[27] An indication of the accuracy of the intercalibration curves (and the specific yield functions) is given by Figure 3, which displays the observed correlation between the 100 g/cm^2 ionization current observed at Thule, Greenland, and the Climax neutron monitor. The interdependence computed in section 5 and displayed in Figure 5 is superposed, after normalization at a Climax neutron rate of 100%. Without any other adjustment the calculated curve provides a good fit throughout the Climax range 80–100%.

[28] As discussed previously, instrumental considerations indicate that the Neher observations retained a good long-term calibration over the whole period 1936–1969. In this section the Forbush ionization data are used to interpolate between the Neher observations, yielding an estimate of the time variation in I(B, t) throughout the interval 1936–1957. In this, the long-term calibration accuracy is provided by the Neher data and the shorter-term time dependence by the Forbush data. All the available Neher data are then used to determine the accuracy of the estimates of I(B, t). Finally, the estimated time dependence of I(B, t) is used to estimate the neutron monitor response that would have been observed throughout the interval 1933–1957.

[29] Let F(t) be the Forbush ground level ionization data for time t. As defined above, I(B, t) is the ionization rate observed at an atmospheric depth of 100 g/cm^2 at Bismarck, North Dakota. The interpolation procedure is applied between the times t_1, t_2. ...t_n, when Neher measurements are available. A linear baseline drift in the F(t) data is assumed between the two end points for each interpolation interval. Then the estimate of I(B, t) is given by

$$I(B,t)_{est} = I(B,t_1) + \beta\{F(t) - F(t_1)\} + D.(t - t_1) \qquad (2)$$

where β is defined below, and the drift coefficient, D, is given by

$$D = \{I(B,t_2) - I(B,t_1) - \beta[F(t_2) - F(t_1)]\}/(t_2 - t_1) \qquad (3)$$

Figure 6 displays the computed time dependence of I(B, t) between 1936 and 1957, based on monthly averages of F(t). Important aspects of these calculations are discussed below.

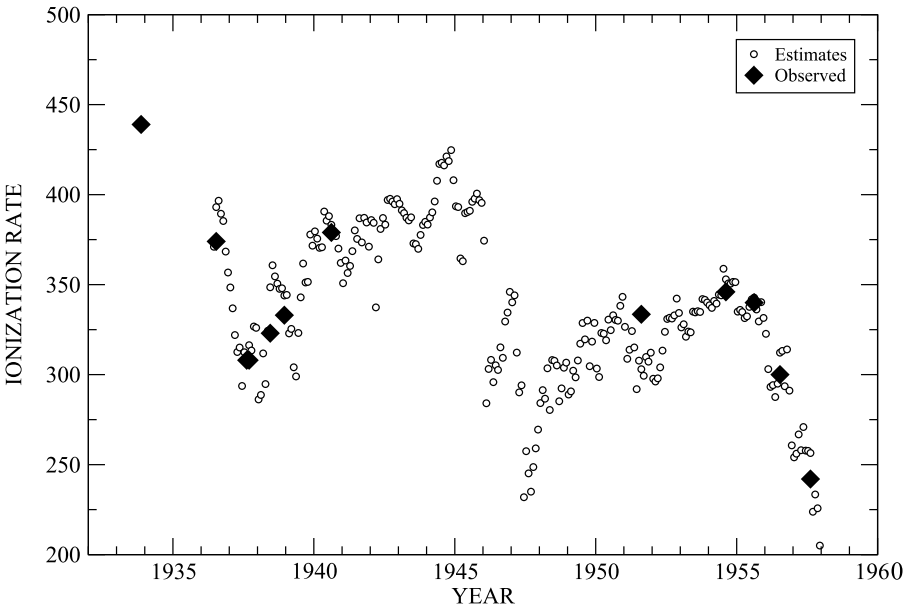

Figure 6. The estimated and observed ionization rates at an atmospheric depth of 100 g/cm^2 at Bismarck for the interval 1933–1957. The open circles are the estimates discussed in the text. The solid diamonds are the direct observations made by *Neher* [1967, and references therein]. Two diamonds overlap in 1937. The ionization rate is given in ion pairs/(cm^3 s atmosphere of air). The long gap in the Neher data after 1941 was due to World War II and its aftermath.

The average values of the ionization observed during 12 separate measurement campaigns between 1933 and 1957 are superimposed upon Figure 6.

[30] The ground-level shielded Compton-Bennett ionization chamber primarily responds to muons, and consequently the ionization current exhibits a dependence upon the temperature throughout the atmosphere (owing to the spontaneous decay of the muons with a mean life of $\sim$2.2 μs). As far as practicable, the monthly data were corrected for this up to 1957 [*Forbush*, 1954, 1958]. To further attenuate the effects of the annual temperature wave, the quantity F(t) is taken as the average of the data from midlatitudes in both the northern and southern hemisphere (Cheltenham and Christchurch, temperature waves out of phase), and from the equatorial station at Huancayo. Note that the long term drifts had been removed from these data by Forbush as discussed above.

[31] The coefficient β is the regression coefficient of the Neher ionization rate upon the average Forbush ionization F(t) outlined above. The functional dependence of these quantities was determined using equation (1) in the same way that the curves in Figure 5 were obtained. Differentiation of the portion of the curve centered on the intensities evident $\sim$1954 yielded β, which was then validated against the observed data for (1) the interval 1954–1957, during which period Neher made annual measurements, and the changes in cosmic ray intensity were large, and (2) the intervals in 1951 and 1954 when many ionization measurements were made during July and August of both years.

[32] The Neher flights only lasted several hours, and the values of I(B, t) are essentially instantaneous measurements, while the Forbush data are averaged over a considerably longer period of time. Further, by operating two ionization chambers at the same location, Forbush determined that the standard deviation of the hourly data was 0.7% [*Lange and Forbush*, 1948]. This large standard deviation would have a considerable impact upon the accuracy of the interpolation. For this reason, the F(t) used to compute the drift coefficient in equation (2) were daily means, and the interpolation end points were chosen to be days on which there were minimal day to day and diurnal variations. The interpolations were made over the intervals 1937–1940, 1940–1954, and 1954–1957.

[33] A preliminary account of this work used annual means for F(t), preliminary values for β, and linear regression relationships [*McCracken and Heikkila*, 2003]. The procedure outlined above is more accurate, especially when the cosmic ray intensity was changing rapidly with time, and the results herein should be used instead of the earlier estimates.

5. Cosmic Ray Intensity During the Sunspot Minimum of 1933

[34] An unshielded Neher ionization chamber was first flown on two manned balloon flights in November 1933 and July 1934. Both occurred prior to the commencement of significant solar activity after the solar minimum of 1933, and they provide the opportunity to make a direct comparison with the ionization measurements made during the sunspot minima of 1954 and 1965. This comparison is complicated by experimental factors, primarily due to the presence of substantial mass in the gondola with the Neher ionization chamber. As a consequence, these data have been disregarded in the literature.

[35] Appendix A reexamines these 1933 data in the light of the time variations observed over the past 50 years and other studies. It is concluded that the 1933 data are consistent with the subsequent behavior of the cosmic rays at Earth, and they are therefore included in the analyses

herein. None of the conclusions are influenced in a significant manner through the use of this data point.

6. Reliability of the Reconstructed Time Dependence 1933–1957

[36] Neher conducted 12 measurement campaigns during the interval given in Figure 6, the resulting values of I(B, t) being superimposed on the reconstruction. For the Neher observations 1937–1957, the standard deviation of $\{I(B, t)_{obs} - I(B, t)_{interp}\}$, the differences between the observations, and the estimated values in Figure 6, was computed to be 16 ions/s, yielding a standard deviation of ~4.5% of the average ionization rates at an atmospheric depth of 100 g/cm^2.

[37] Neher estimated that the standard deviation of his data was ~0.5–1%. It can be shown that to a good degree of approximation the standard deviation of $\{I(B, t)_{obs} - I(B, t)_{interp}\}$ is

$$\sigma\left\{I(B,t)_{obs} - I(B,t)_{interp}\right\} = \left\{2x\left[\sigma\left\{I(B,t)_{obs}\right\}\right]^2 + \beta^2.[\sigma(F(t))]^2\right\}^{0.5}$$

and this shows that the 4.5% standard deviation for $\{I(B, t)_{obs} - I(B, t)_{interp}\}$ is consistent with a 0.4% standard deviation of the monthly averages, F(t). There will be residual errors in F(t) due to temperature effects, and nonlinear sensitivity changes due to operator induced errors, and a standard deviation of 0.4% is in accord with expectations. We conclude that the errors in the data after correction for the long-term changes are primarily due to the statistical and other errors in the monthly Forbush data and are small compared to the long-term corrections (~20%) provided by the Neher data.

[38] While Neher and Forbush continued their observations until 1969, the Forbush data were not subjected to the same high degree of scrutiny and calibration after 1957 as was done for the publication by *Forbush* [1958]. For this reason, the data in the interval 1958–1969 could not be used with confidence in the analyses in this paper.

7. The ^{10}Be Record, 1428–1950

[39] As discussed in the introduction, *Beer* [2000] has pointed out that the sequestration of ^{10}Be in polar ice constitutes a natural neutron monitor, whose record extends far into the past. Figure 4 shows that the specific yield function of ^{10}Be extends to lower energies than those of the Climax and sea level neutron monitors. Stated differently, the response function of the ^{10}Be peaks at a lower energy (1–2 GeV/nucleon) than in the case of the sea level neutron monitor (6 GeV/nucleon), as deduced by *McCracken* [2004]. As a consequence, for the period 1951–present, the ^{10}Be data exhibit percentage changes that are approximately twice those in the instrumental neutron record. The pronounced nonlinearity evident in Figure 5 means that this factor is ~3.5 for periods near a Gleissberg minimum, i.e., for periods such as 1890–1900 when the cosmic ray intensity at Earth was substantially higher than during the space age.

[40] Using 22-year average data, *McCracken et al.* [2004a] have shown that there is good agreement between the independent measurements of ^{10}Be from the Arctic and the Antarctic for the interval 1433–1958 (correlation coefficient = 0.87). They inferred that the standard deviations of the individual 22-year averages are ~4.4%, compared to the >40% long term changes in the data. This provides confidence that the ^{10}Be data provides a reasonable record of the century-scale changes in the galactic cosmic radiation.

[41] The South Pole data are 8-year samples, and the Nyquist theorem indicates that they will be unsuitable for study of the 11-year variations in the cosmic radiation [*McCracken*, 2004]. The Dye 3, Greenland [*Beer et al.*, 1990] ^{10}Be data were sampled annually, and they allow the 11-year variation to be studied. The measurement errors in the annual data are estimated to be 4–10% [*Beer et al.*, 1990]; in addition there are atmospheric effects that vary from year to year (called system effects in the glaciological literature). To minimize these errors, the data were passed through a (1, 4, 6, 4, 1) time series (binomial) filter to remove high-frequency noise, yielding a standard deviation of <6% for short-term fluctuations. This filter was chosen because it completely attenuates the atmospheric effects due to the biannual North Atlantic Oscillation, while only reducing the amplitude of the 11-year cycle by 15%.

[42] The strength of the geomagnetic field decreased by a significant amount over the period of this study, thereby reducing the cutoff rigidities; this effect was removed from the ^{10}Be data as described by *McCracken et al.* [2004a]. In addition, large solar energetic particle (SEP) events make significant contributions to the ^{10}Be concentration [*McCracken et al.*, 2001a]. Using neutron observations made during the solar cosmic ray event of 23 February 1956, *McCracken et al.* [2001a] estimated that the ^{10}Be production rate was 3.1×10^2 atoms/g for a SEP fluence of 10^9 cm^{-2}. Further, *McCracken et al.* [2001b] tabulated 70 SEP with >30 MeV fluences $>2 \times 10^9$/cm^2 in the period 1561–1950 based on the high-resolution nitrate signal in polar ice. These two results were used together to estimate the year by year production of ^{10}Be by solar cosmic radiation and to subtract it from the observed ^{10}Be data [see *McCracken et al.*, 2001a]. This calculation showed that there is a sporadic contribution to the ^{10}Be concentration due to solar cosmic rays (~5–15% at times of frequent solar energetic particle (SEP) events) that is greatest during periods of low long-term solar activity [*McCracken et al.*, 2001a, 2004b]. The majority of this solar production occurs during the solar cycle and has the effect of reducing the amplitude of the 11-year modulation of the cosmic rays. In addition, however, the calculations show that the solar cosmic rays can result in ≤15% overall enhancements of the ^{10}Be signal during the Grand Minima (1700, ~1810, ~1895). The nitrate data are estimated to miss ~25% of all large SEP [*McCracken et al.*, 2001b]; there will be event to event variations in the rigidity spectra of the solar cosmic rays and consequently, the solar corrections may be underestimated by ~3%. These sporadic residual errors are less than the estimated ^{10}Be measurement errors and will not make a significant contribution to either the long-term variations or the output of the (1, 4, 6, 4, 1) time series (binomial) filter. Note however that no high-resolution nitrate data exist for the Spoerer Minimum, and therefore there may be a solar contribution during that period. It is estimated to be relatively small (<5%) by analogy to

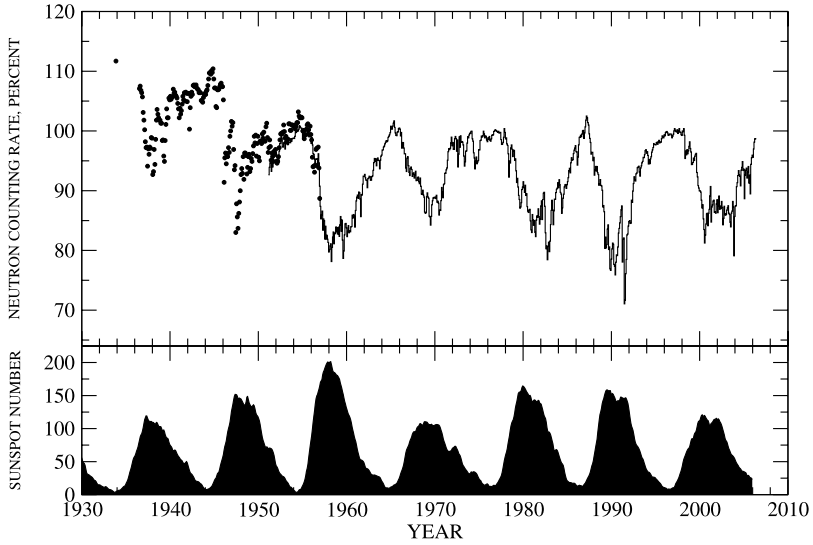

Figure 7. The observed and estimated monthly Climax neutron counting rates (connected line and solid dots, respectively), and the international sunspot number, 1933–2005. The estimates for the interval 1936–1957 were made as detailed in the text. Both the observed and estimated counting rates were normalized to 100% in 1954.

the Maunder Minimum, for which the nitrate data were available. More recently, *Usoskin et al.* [2006] and *Webber et al.* [2007] have used numerical ^{10}Be production models to refine the earlier experimentally based estimates of the ^{10}Be yield; however, the partial nature of the nitrate record and the variability of the spectra remain the more significant causes of residual solar contamination in the corrected ^{10}Be record.

[43] In summary, the ^{10}Be data contain residual statistical, meteorological, and solar cosmic ray components in addition to the galactic cosmic ray signal. The standard deviations of 22-year averages are ~4.4% for long-term changes in the data and <6% for the output of the (1, 4, 6, 4, 1) filtered data. These are to be compared with the ~40% long-term changes and the ~25–35% 11-year variations in the filtered data. The filtered ^{10}Be data therefore provides a relatively good representation of the time dependence of the galactic cosmic radiation with a signal to noise ratio of ~8:1, at both 11-year and longer-term timescales. These standard deviations indicate, however, that there will be occasional meteorological and solar components that will distort the overall record. Thus one 11-year cycle out of 20 will contain a 12% atmospheric and solar component superimposed on the 25–35% 11-year variation. One out of three may contain 6% meteorological or solar components.

[44] We take the view that this level of contamination of the record is acceptable provided that the presence of occasional meteorological and solar cosmic ray noise is kept in mind. The acquisition of several more annual ^{10}Be records, high-resolution nitrate records from both polar caps, and analysis in combination with the ^{14}C record will allow the noise contributions to be reduced further in the future.

8. Intercalibrated Cosmic Ray Intensity, 1428–2005

[45] Using the nonlinear Neher versus Climax intercalibration curve from Figure 5 and the data in Figure 6, the monthly Climax counting rates were estimated for the interval 1933–1956. These estimates, together with the observed counting rates, 1951–2005 are displayed in Figure 7. They are also given in Table 1. On the basis of the standard deviation of 4.5% derived for the interpolated Neher record (section 6), and Figure 5, the standard deviation of the Climax estimates for 1933–1956 is computed to be ~2%.

[46] Using the intercomparison graph in Figure 5, the (1, 4, 6, 4, 1) filtered ^{10}Be data were used to estimate the pseudo-Climax neutron monitor counting rates (the effects of geomagnetic change and solar cosmic rays having been removed as discussed in section 7). Figure 8 displays the estimated and observed neutron monitor response for the period 1428–2005. The data for 1428–1930 are based on the ^{10}Be data; the interval 1933–1951 is derived from the Forbush and Neher data as presented in Figure 7, while 1951–2005 is the neutron monitor data record from Climax, Colorado.

[47] As discussed in section 7, solar cosmic rays enhance the ^{10}Be concentration during the Grand Minima by 5–15%. Converted to the equivalent filtered (1, 4, 6, 4, 1) pseudo-Climax counting rate, the solar components were 1.5% centered on 1700, 1.9% for 1813, and a decade-long episode between 1890 and 1900 that peaked at 7.0% in 1896. In the latter case, the solar component changed the nature of the 11-year variation to a very substantial degree [*McCracken et al.*, 2001a].

[48] Previous extrapolations of the neutron monitor data into the past have been based on two different methodologies. Some have been based on using linear regression, and as discussed above and by *Mursula et al.* [2003], this overlooks the nonlinearities evident in Figure 5. Others have used an indirect method that first estimates the modulation potential using a nonlinear inversion and then uses it to estimate the cosmic ray intensity [*Usoskin et al.*, 2002]. The intercalibrated neutron record (the pseudo-Climax record) avoids both approximations, depending on the accuracy of the specific yield functions, which are now

Table 1. Estimated Climax Neutron Monitor Counting Rates, Based on the *Neher* [1971] and *Forbush* [1958] Ionization Chamber Data[a]

	Jan	Feb	Mar	Apr	May	Jun	Jul	Aug	Sep	Oct	Nov	Dec	Mean
1936							107.1	107.5	106.8	106.4	105.7	103.1	106.1
1937	101.8	100.2	98.2	97.2	97.3	94.1	97.0	96.1	97.3	97.1	98.9	98.8	97.8
1938	92.7	93.2	96.9	94.4	98.6	101.8	103.6	102.8	102.2	101.8	101.8	101.3	99.3
1939	101.3	98.4	98.5	95.8	94.9	98.4	101.1	103.7	102.2	102.2	105.5	105.2	100.6
1940	105.8	105.3	105.6	105.7	107.0	106.3	106.5	106.0	105.8	105.5	104.6	103.7	105.7
1941	102.2	103.8	102.8	103.4	104.5	105.8	105.2	106.4	105.0	106.5	106.3	104.9	104.7
1942	106.3	106.3	100.3	103.9	105.8	106.5	106.1	107.6	107.7	107.4	107.5	107.7	106.1
1943	107.2	107.0	106.9	106.4	106.5	106.4	105.1	105.0	104.8	105.6	106.1	106.3	106.1
1944	106.1	106.7	106.9	107.6	108.7	109.7	109.8	109.5	110.1	109.8	110.4	108.7	108.7
1945	107.2	107.2	104.1	103.9	106.9	106.9	107.0	107.4	107.8	108.0	107.5	107.4	106.8
1946	105.2	91.4	95.5	96.3	94.5	95.9	95.7	97.2	96.4	99.1	100.0	101.6	97.4
1947	100.8	101.4	96.9	93.5	94.2	83.0	87.8	85.6	83.7	86.2	88.1	90.0	90.9
1948	92.7	93.7	92.9	95.7	91.9	96.3	96.3	95.9	92.8	93.9	95.7	96.1	94.5
1949	93.2	93.7	95.4	94.9	96.2	97.5	99.1	98.0	99.3	95.8	97.9	99.1	96.7
1950	95.6	95.0	98.3	98.3	97.9	99.5	98.8	99.8	98.3	98.3	100.7	101.3	98.5
1951	98.9	96.4	97.2	98.5	97.4	95.1	96.3	95.7	94.9	96.6	96.1	96.9	96.7
1952	94.9	94.6	94.9	95.7	97.2	98.5	99.5	99.6	99.5	99.8	101.0	99.9	97.9
1953	98.8	99.1	98.2	98.7	98.6	101.2	101.2	100.1	100.1	101.0	101.0	100.9	99.9
1954	100.7	100.4	101.0	100.7	101.4	101.4	103.2	102.5	102.2	102.2	102.3	102.2	101.7
1955	100.0	100.1	98.7	99.3	99.4	100.3	101.0	101.2	100.2	99.3	100.8	99.4	100.0
1956	98.5	95.6	94.0	94.1	93.1	94.3	96.9	97.1	94.1	97.3	93.8	88.7	94.8

[a]The normalization to the observed data was for the year centered on 1 August 1954, being the highest intensities during that sunspot minimum. Here, 100% corresponds to a Climax hourly counting rate of 4208. As discussed in the text, the standard deviation of these estimates is estimated to be 2%.

well known. As a consequence, the intercalibrated record developed here is expected to be the most satisfactory for the study of the long-term characteristics of the cosmic ray intensity.

[49] Figure 8 exhibits short-term time variations that are similar to those observed in the instrumental record and longer-term variations that clearly reflect the Spoerer, Maunder, and Dalton minima. As discussed above, the

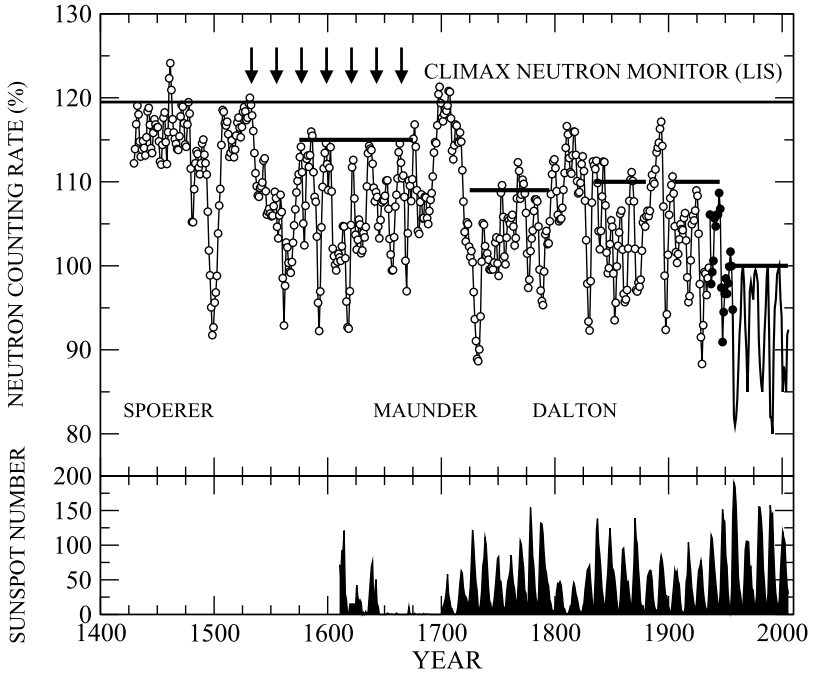

Figure 8. The observed and pseudo-Climax neutron counting rate and the international sunspot number. The annual ^{10}Be data (1428–1930) have been averaged with a (1, 4, 6, 4, 1) binomial filter prior to plotting; the other data are annual averages. The line Cnm(LIS) is the estimated value of the pseudo-Climax counting rate in the absence of any solar modulation (see text). The heavy lines indicate the levels of ''residual modulation'' during the four Gleissberg maxima. The arrows between 1533 and 1686 are at 22-year intervals and demonstrate that the cosmic radiation was under solar control throughout this interval. The effects of the long-term change in the geomagnetic dipole, and the production of ^{10}Be by solar cosmic rays, have been removed from these data. The high point at 1465 is discussed by *McCracken et al* [2004a].

Table 2. Comparison of the Intercalibrated Climax Neutron Monitor Averages for Various Periods Between 1428 and 2005[a]

Interval	Average	Residual Modulation
Whole interval (1428–1933)	108.0%	
	Low Modulation	
Spoerer Minimum (1428–1473)	116.0%	
Maunder Minimum (1645–1715)	110.9%	
	Gleissberg Maxima of Enhanced Solar Activity	
1540–1644	106.9%	115%
1725–1760	100.9%	109%
1825–1880	104.4%	110%
1900–1933	103.2%	110%
Modern epoch (1954–2005)	92.3%	100%

[a]The intensities are in percent, relative to 100% in August 1954. The residual modulations are shown as solid lines in Figure 8.

^{10}Be data still contain some short- and long-term variations due to climate change [*Lal*, 1987], year to year atmospheric effects, solar cosmic rays, and measurement and timing errors (standard deviation ~6%). These imply a noise component in the pseudo-Climax record prior to 1933 with a standard deviation of ~3%.It is clearly desirable that several more ice cores should be sampled at yearly intervals to assess such system errors and to improve the accuracy of the intercalibrated record.

9. Characteristics of the Cosmic Ray Variations, 1428–2005

[50] The intercalibrated neutron records in Figures 7 and 8 are now used to discuss the characteristics of the longer-term variations in the cosmic ray intensity at Earth. In particular, they are used to make a detailed comparison between the variations observed during the instrumental era 1933–2005, and the cosmogenic record for ~500 years prior to 1933. For brevity, the annotations SSmin and SSmax are used to indicate the minima and maxima of the solar cycle. As discussed in section 4, Cnm(LIS) is used to denote the pseudo-Climax neutron monitor counting rate when the local interstellar cosmic ray spectrum is incident on Earth (i.e., φ = 0 MV).

[51] Fourier analyses of the sunspot, auroral, and cosmogenic data record yield a periodicity in the vicinity of 80–95 years called the Gleissberg periodicity. The Spoerer, Maunder, and Dalton minima, and the period of low solar activity, 1890–1910, are referred to collectively as the Gleissberg minima and the intervals between are referred to as the Gleissberg maxima. We use that convention here. Note, however, that the cosmic ray intensity is high when solar activity is low. That is, the long-term variations in the cosmic radiation are at maxima during the Gleissberg minima, and vice versa.

9.1. Reduced Cosmic Ray Intensity, 1954–2005 AD

[52] Using 22-year average data, *McCracken et al.* [2004a] concluded that the interval 1954–2004 exhibited one of the lowest values of cosmic ray intensity in the past 1000 years. Similar conclusions were reached by *Usoskin et al.* [2003] and *Muscheler et al.* [2007]. We now examine this result further, using the annual data displayed in Figure 8. Table 2 presents the mean values of the data in Figure 8 for several periods of interest. As stated above, Cnm(LIS) = 119.5% in the absence of any modulation. For the two "Grand Minima," the Spoerer and Maunder Minima, the averages are 116.0% and 110.9%, respectively. Figure 8 shows that there was sustained modulation throughout these periods, as will be discussed later, and both averages are substantially below the "no modulation" value, although there are periods of several years at a time when the values approximate the "no modulation" figure as discussed by *McCracken et al.* [2004a].

[53] The first three "Gleissberg Maxima" in Table 2 correspond to the extended periods of solar activity between the Spoerer, Maunder, and Dalton "Grand Minima," and the Gleissberg Minimum of 1900. The fourth is the period between 1900 and the sunspot minimum of 1933. The averages of all four intervals lie in the range 100–107%. The average for the whole of the 517-year interval 1428–1933 is 108.0%. That is, for the period 1428–1933, the average values of the intercalibrated neutron record range between 116% and 100%, while the long-term average is 108.0%.

[54] Consider now the entry in Table 2 for the modern era since 1954. The average value is 92.3%, which is ~16% below the average for the whole interval 1428–1933 AD. It is ~10% below the averages of the four Gleissberg maxima in Table 2. Figures 7 and 8 show that starting in 1954; the SSmin value remained consistently at ~100% for five sunspot minima. At no time during the previous ~500 years did the SSmin intensity fall below 105% (allowance being made for the attenuation of the 11-year signal in the (1, 4, 6, 4, 1) filter). While the pseudo-Climax record exhibits values below 95% on seven isolated occasions in the previous ~500 years, it was consistently lower than 90% for each of the sunspot maxima from 1954 onward.

[55] In summary, the period since 1954, comprising the "neutron monitor" and the "space" eras, exhibits a mean intensity and a depth of 11-year modulation that had not occurred in the previous ~500 years. While there were isolated occasions when the intercalibrated intensity approximated 90% in the past, as previously established by *McCracken et al.* [2004a] using 22-year averages of the cosmic ray data, the depth of modulation, and the persistency over 5 solar cycles is unique. We note however that the cosmic radiation was strongly modulated between 1100 and 1220, usually called the Medieval Maximum [*McCracken et al.*, 2004a]. No annual ^{10}Be data are presently available for that period; the 22-year ^{10}Be data suggest that when available they may show a depth and persistence of modulation similar to that observed since 1954.

9.2. Comparison of the Residual Modulation Between Gleissberg Cycles

[56] The term "residual modulation" refers to the manner in which the cosmic ray intensity remains depressed below the LIS value between successive solar cycles. This is most clearly illustrated by the period 1954–2005 in Figures 7 and 8, where the Climax intensity consistently recovers to an approximate asymptote of ~100% after each solar cycle, well below the Cnm(LIS) value of 119.5%. Contemporary satellite measurements show that the strength of the heliospheric magnetic field (HMF) has exhibited an approximate SSmin asymptote of 5.2 nT since 1965. The substantial

amount of ''residual modulation'' during these sunspot minima is consistent with these values of HMF, the observed solar wind speed, and the cosmic ray transport equation of *Parker* [1965].

[57] The heavy lines in Figure 8 are estimates of the residual modulation during the four intervals associated with the Gleissberg periods of enhanced solar activity; these intensities are entered into the third column of Table 2. From this, and from examination of Figure 8, it is clear that the amount of residual modulation increased substantially (i.e., the intensity decreased) between the Gleissberg maximum of 1540–1644 and the two subsequent maxima and that it increased further between the SSmin of 1944 and 1954. This implies that there was a systematic change in the heliospheric environment at sunspot minimum over the past 580 years, as discussed in section 9.4.

[58] It is instructive to compare the data from the Spoerer Minimum and the subsequent Gleissberg period of solar activity, 1540–1644. Note that the residual modulation during the latter period is a minor effect compared to the 11- and 22-year modulation. On the basis of these data alone, the residual modulation would not be considered significant. Its significance only becomes apparent in the context of the larger levels of residual modulation evident in the subsequent Gleissberg cycles. This will be discussed further in the next section.

9.3. Strength of the Gleissberg Solar Cycle, 1540–1645

[59] The Maunder Minimum (1645–1715) is well known as a period of low solar activity when almost no sunspots were observed (Figure 8). It coincided with a period of very high production of cosmogenic radionuclides. The Maunder minimum together with the earlier Spoerer Minimum (1420–1540) are the most profound ''Grand Minima'' in the cosmogenic and auroral records for the past 1000 years [*McCracken et al.*, 2004a, and references therein]. Both were of long duration; in each there were periods of several years at a time when the cosmic ray intensity approximated the ''no modulation'' figure (Cnm(LIS) = 119.5%). The sunspot record (Figure 8) shows that the two Gleissberg maxima (1715–1810) and (1810–1889) exhibited similar levels of solar activity (i.e., similar sunspot cycle amplitudes). Subsequent to that, solar activity has been greater from 1944 onward. As discussed in section 9.1 and shown in Table 2, the mean cosmic ray intensities are consistent with these observations.

[60] There is only a fragmentary sunspot record for the Gleissberg Maximum, 1540–1645, and this is inadequate to allow comparison of the solar activity during that cycle with the later ones. In view of it being between the two most profound Grand Minima, it is desirable to know whether the overall solar activity was also reduced during this interval. That is, was the solar activity throughout the whole period 1420–1715 anomalously low? Alternatively, was the level of solar activity (1540–1645) similar to the later periods, being ''turned off'' for longer periods and more profoundly during the Spoerer and Maunder Minima than during the later Minima (e.g., Dalton)? The cosmogenic data allows this question to be answered and demonstrates a methodology that will permit the development of the Grand Minima to be investigated, when annual or similar data are available for the period 1000–1428 AD.

[61] As discussed in sections 9.1 and 9.2 and as is evident in Figure 8, the cosmic ray modulation effects during the interval 1540–1645 were less pronounced than in the Gleissberg Maxima after the Maunder Minimum. This difference is apparent in the second and third columns of Table 2. The second column shows that there was less average modulation; that is, the average intensity was higher (106.9%) compared to the later cycles. The third column presents more striking evidence. As discussed in section 9.2, the residual modulation effect (1540–1645) was about 50% of those in the subsequent Gleissberg cycles and only about 25% of that in the modern era (1954–date). Over the timescale of the 11-year cycle, there is an approximately inverse relationship between the cosmic ray intensity and solar activity (measured in terms of the sunspot number), as is evident from Figure 8. That is, the lower the peak sunspot number, the higher the cosmic ray intensity. On the basis of the evidence in the second and third columns of Table 2, it is estimated that the peak sunspot numbers during the Gleissberg cycle 1540–1645 were approximately half those in the subsequent two cycles.

[62] Table 2 therefore shows that solar activity was relatively low throughout the whole interval 1428–1715 and not just during the Grand Minima. Throughout the whole period, there was little residual modulation, and the 11- and 22- year modulation events all commenced from a level close to Cnm(LIS).

9.4. The 2300 Year Periodicity in the Cosmic Ray Intensity

[63] Power spectra studies of the cosmogenic ^{10}Be and ^{14}C data for the past ~10,000 years have identified a periodicity in the vicinity of ~2300 years, and the occurrence in both data sets shows that they are not due to meteorological effects [*Damon and Sonett*,1991; *Beer et al.*, 1988]. Examination of the cosmogenic records [e.g., *Peristykh and Damon*, 2003, Figure 2] shows that short episodes of Grand Minima such as the Spoerer, Maunder, and Dalton minima in Figure 8 have occurred at roughly 2300 year intervals over the past 10,000 years, with long intervals (up to 2000 years) in between without any Grand Minima. That is, the cosmogenic data show that the Sun has exhibited long periods of extended activity, the periods of low solar activity evident from the sunspot record being a relatively uncommon but repetitive phenomenon. Figure 2 of *Peristykh and Damon* [2003] shows that the most recent ''cluster'' of Grand Minima in the past 10,000 years was centered on the Spoerer and Maunder minima (~1550 AD), suggesting that this was the maximum of the 2300 year periodicity in cosmic ray intensity previously detected in the power spectra analyses.

[64] The data in Figure 8 show that there has been a long-term, systematic change in the heliospheric environment over the past 580 years. Thus (1) the Grand Minima have become shorter and less profound from the Spoerer minimum (longest) to the Dalton minimum (shortest), (2) the residual modulation has steadily increased, and (3) the average cosmic ray intensity has steadily decreased. We propose that these changes constitute the first quarter cycle of the ~2300 year periodicity following the maximum in ~1550 AD and that the above three properties are characteristic of that periodicity. The companion paper estimates

that the strength of the heliomagnetic field increased steadily throughout this period.

9.5. Long-Term Changes in the Cosmic Ray Intensity, 1889–1954 AD

[65] Figures 7 and 8 show that the cosmic ray intensity at sunspot minimum decreased by ~9% between 1889 and 1902. It then remained essentially constant (at ~110% relative to 1954) for the sunspot minima of 1913, 1923, 1933, and 1944. The SSmin intensity then decreased by ~10% between 1944 and 1954. Thereafter the SSmin intensity remained close to 100% for the 5 solar cycles until the present. Clearly, the majority of the long-term change occurred as two downward steps, between 1889 and 1901 and between 1944 and 1954. Good geomagnetic and solar observations exist for this period, offering the promise of using this period to understand the interactions between solar activity, and the heliospheric environment, to a greater degree.

[66] The *Parker* [1958] theory of the solar wind shows that some of the Sun's coronal magnetic fields will be "frozen into" the solar plasma, this being the source of the heliospheric magnetic field. Assuming that the flux of magnetic field away from the Sun is determined, in part, by the magnetic flux in the sunspot groups, several workers have used the sunspot record to model the temporal dependence of the heliomagnetic field (HMF) [*Solanki et al.*, 2000; *Wang et al.*, 2002; *Schrijver et al.*, 2002]. *Usoskin et al* [2002] have shown that the modeled HMF is in agreement with the observed cosmogenic ^{10}Be data. Others [*Lockwood et al.*, 1999] have used characteristics of the disturbances in the geomagnetic field to estimate the strength of the HMF near Earth. In general, these models have predicted an increase in the strength of the heliomagnetic field between 1889 and 1954. The model of *Schrijver et al.* [2002], in particular, predicts a relatively small increase in the solar magnetic flux between ~1890 and 1900, relative constancy between 1902 and 1935, a large increase between 1935 and 1955, followed by fluctuations about a high "plateau" value, substantially greater than at any time between 1890 and 1935. That is, their model exhibits a "two step" behavior similar to that of the cosmic ray intensity but of the opposite phase.

[67] The cosmic ray transport equation [*Parker*, 1965] has been shown to provide an accurate description of the cosmic ray variations since 1951. The strength of the HMF plays a key role in this equation, with, in general, the cosmic ray intensity varying inversely as the strength of the HMF. This is consistent with all of the abovementioned studies. Further, the "two step" behavior in the cosmic ray intensity is consistent with the synchronous "two step" increases in the HMF, as estimated by *Schrijver et al.* [2002]. *Caballero-Lopez et al.* [2004] have developed a procedure to invert the cosmic ray data, yielding estimates of the strength of the HMF, and the companion paper uses their procedure to invert the data in the intercalibrated record, 1428–2005 [*McCracken*, 2007].

10. Summary and Conclusions

[68] Attention has been drawn to the fact that the Forbush ionization chamber data, 1936–1957, were detrended to remove long-term variations. As a consequence, those data are unsuitable for normalization of the cosmogenic radionuclides to the modern instrumental era. As they stand, they are also unsuitable for study of the long-term cosmic ray intensity or for the estimation of the changes in the heliomagnetic field.

[69] The specific yield functions of five different species of cosmic ray data were used to compute their several interrelationships. It was shown that the interrelationships are significantly nonlinear and that the use of linear regression relationships will introduce large errors in converting from one data type to another.

[70] The high-altitude ionization chamber data obtained by *Neher* [1971, and references therein] were calibrated against terrestrial standards, and they exhibit a ~27% decrease between 1933 and 1965. The Forbush data were used to interpolate between the isolated Neher observations, yielding an estimate of the monthly variations that would have been observed by the Neher ionization chambers, 1933–1957. This shows that the cosmic ray intensity decreased by a large degree between 1944 and 1954. The nonlinear relationship (Neher ion to Climax neutron) was then used to estimate the neutron monitor response for the interval 1933 and 1954 given in Figure 7.

[71] The effect of the long-term secular change in the geomagnetic field was then removed from the ^{10}Be data from Dye 3, Greenland, for the period 1428–2005, as was an estimate of the ^{10}Be produced by solar cosmic rays (1572–1933). The presence of residual errors due to measurement and statistical fluctuations and uncompensated meteorological and solar cosmic ray contributions were then discussed. The nonlinear interpolation relationship (Figure 5) was then used to convert the ^{10}Be data into the pseudo-Climax record, discussed previously. This new, intercalibrated record allows the cosmic ray intensities to be compared throughout the period 1428–2005.

[72] Our calculations show that solar cosmic rays increased the (1, 4, 6, 4, 1) filtered ^{10}Be concentration during the Grand Minima by 5–15%. Converted to the equivalent filtered (1, 4, 6, 4, 1) pseudo-Climax neutron counting rate, the solar components were 1.5% centered on 1700, 1.9% for 1813, and a decade long episode between 1890 and 1900 that peaked at 7.0% in 1896.

[73] The pseudo-Climax record shows that the period since 1954 exhibited a consistency of strong cosmic ray modulation that had not occurred during the previous ~500 years. While there were isolated occasions when the consolidated intensity decreased to the levels observed since 1954, the depth of modulation and the persistency over 5 solar cycles is unique.

[74] The "residual modulation" of the cosmic radiation increased from a low level for the Gleissberg maximum 1540–1645, to an intermediate level for the next two Gleissberg maxima, and was greatest for the period after 1944. That is, there has been a long-term increase in the efficiency of the cosmic ray modulation at sunspot minimum over the past 580 years.

[75] It is suggested that the steadily increasing level of cosmic ray modulation and the progressive shortening of the Grand Minima since 1428 represent the first quarter of the ~2300 year periodicity previously identified in the cosmogenic data for the past 10,000 years.

[76] Consideration of the average cosmic ray intensities, and the amount of residual modulation, led to the conclusion that the solar activity during the Gleissberg cycle 1540–1645 was approximately 50% of that of the two following cycles and about 25% of the modern era. This indicates that the solar activity was anomalously low throughout the whole period 1428–1715, including the Spoerer and Maunder Minima and the Gleissberg cycle in between.

[77] It was also shown that the cosmic ray intensity decreased by ~19% between 1889 and 1954 in two steps, the first being a 9% decrease between 1889 and 1901 and the second a decrease of 10% between 1944 and 1954. It is noted that the mathematical model of *Schrijver et al.* [2002] yields upward steps in the strength of the heliomagnetic field at those times. The two step nature of both records is consistent with the cosmic ray transport equation of *Parker* [1965].

[78] In addition, this work has provided the estimates given in Figure 8, and Table 1, which will allow other cosmogenic radionuclide data to be normalized to the neutron monitor epoch that commenced in 1951.

Appendix A: Cosmic Ray Intensity, 1933

[79] As outlined in section 5, the first Neher ionization chamber was flown in 1933–1934. Experimental factors complicate the use of those data; it is the purpose of this appendix to show that the results of the 1933 flight are reliable and can be used as the first member of the instrumental cosmic ray record.

[80] The instrument was similar to the chamber described by *Millikan and Cameron* [1928] and was used in later years as a calibration standard [*Neher and Anderson*, 1964] for the "free-flying" instruments discussed in section 3. It was first flown on a manned balloon ("The Century of Progress") that flew from Akron, Ohio (geomagnetic cutoff 1.73 GV) to Bridgetown, New Jersey (1.9 GV) carrying two men and 11 different experiments [*Compton*, 1934]. It was flown again on the "Explorer 1" balloon in July 1934, from Rapid City, South Dakota with a three-man crew (see *DeVorkin* [1989] for details of these flights). There was a substantial amount of mass in the gondola on both occasions, in addition to the crews. Nevertheless, there was good consistency between the data from the two flights [*Bowen et al.*, 1937].

[81] In August 1937, the ionization rate measured with a small unmanned balloon at Saskatoon, Manitoba was ~30% lower than the rate measured during the balloon flights in 1933–1934. At the time, it was widely thought that the cosmic radiation at Earth was invariant with time, and it appears from the literature that no consideration was given to the possibility that the cosmic ray intensity had decreased with the increase in solar activity between 1933 and 1937. Consequently, the 30% discrepancy caused the 1933–1934 observations to be regarded with suspicion. In addition to Neher's unshielded chamber, both balloons carried small shielded ionization chambers (7.5 cm thickness of lead shot), in addition to the crew of two/three, and other mass such as sand ballast, and other experiments. The discrepancy led to the valid concern that nuclear reactions in the lead shield, and other mass on the balloon, had generated secondary particles that were the cause of the high values observed in 1933–1934, and the 1933–1934 measurements were disregarded. The reliability of the observations is reassessed in the following paragraphs in the light of modern knowledge.

[82] The 1933–1934 observation, after correction to the geomagnetic cutoff of Bismarck, is plotted in Figure 6. As outlined above, the ionization rate was measured to be ~30% less 3 1/2 years later at Saskatoon in August 1937. Between those dates, the sunspot number had increased from 0.6 to 138. Modern experience shows that the neutron monitor counting rate has decreased by between 14 and 23% during the first 3 1/2 years of all solar cycles since 1954. On the basis of the intercalibration curve in Figure 5, this implies reductions of 23–38% in I(B,t). The ~30% reduction observed between 1933 and 1937 is therefore consistent with these more recent observations.

[83] Neher considered this type of problem again, in analyzing the data from one of his ionization chambers flown on the Mariner 2 spacecraft in 1962 [*Neher and Anderson*, 1964]. They showed that nuclear reactions in the mass of the midcourse motors and other equipment on the spacecraft representing up to 60 g/cm^2, and subtending a solid angle of 0.82 steradians at the ionization chamber, would result in an increase <0.2% in the observed ionization rate. In the case of the 1933–1934 observations, the available evidence [*DeVorkin*, 1989] indicates that the solid angle subtended by the shielded ionization chamber was 0.025 steradians, and the other mass (including the crew) would have subtended a solid angle comparable to that in the case of the Mariner spacecraft.

[84] Nevertheless, it is clear that the 1933 observations were influenced by two opposing effects that were not present in the Neher observations from 1936 onward. They are (1) a reduction in ionization current due to absorption of the electron and muon components in the 1 g/cm^2 skin of the gondola and (2) an increase due to the secondaries from nuclear interactions in the mass in the instruments and the crew. In view of the uncertain geometry within the gondola (e.g., the unknown positions of the crew), the 1933 observation is taken as an approximation to the ionization that would have been observed by a free-flying ionization chamber as used from 1936 onward.

[85] Consider now the estimated neutron counting rate for 1933 in Figure 7, derived from the manned balloon flight in November 1933. It is 7% higher than the neutron counting rate estimated for July 1936, 32 months later. The 1933 sunspot minimum corresponded to comic ray modulation characterized by $qA > 0$, as did the sunspot minima of 1954, 1976, and 1997. In those cases, the neutron monitor intensity decreased by 15%, 10%, and 16%, respectively, in the first 32 months of the subsequent cycles. That is, the estimated 7% decrease in neutron monitor counting rate from 1933 to 1936 is broadly consistent with the neutron data obtained during the onset phases of the subsequent three $qA > 0$ sunspot cycles. This consistency with the later $qA > 0$ cycles, and the calculations of *Neher and Anderson* [1964] outlined above, lead to the conclusion that the ionization rates observed in 1933 were not greatly influenced by the mass in the balloon gondola. On the basis of these several reasons, it is concluded that the estimate for 1933 in Figure 7 and Table 1 is reliable and that it has a

standard deviation similar to those of the other data in Figure 7.

[86] **Acknowledgments.** The research at the University of Maryland was supported by NSF grant ATM 0107181. The Climax neutron monitor data were supplied by the University of New Hampshire, supported by NSF grant ATM-9912341. This research was also supported by the Swiss National Science Foundation. Support by the International Space Science Institute, Bern, Switzerland, is gratefully acknowledged.

[87] Zuyin Pu thanks the reviewers for their assistance in evaluating this paper.

References

Beer, J. (2000), Neutron monitor records in broader historical context, *Space Sci. Rev.*, *93*, 107–119.

Beer, J., U. Siegenthaler, G. Bonani, R. C. Finkel, H. Oeschger, M. Suter, and W. Wolfli (1988), Information on past solar activity and geomagnetism from ^{10}Be in the Camp Century ice core, *Nature*, *331*, 675–679.

Beer, J., et al. (1990), Use of ^{10}Be in polar ice to trace the 11-year cycle of solar activity, *Nature*, *347*, 164–166.

Bowen, I. S., R. A. Milliken, and H. V. Neher (1937), The influence of the Earth's magnetic field on cosmic-ray intensities up to the top of the atmosphere, *Phys. Rev.*, *52*, 80–88.

Caballero-Lopez, R. A., H. Moraal, K. G. McCracken, and F. B. McDonald (2004), The heliospheric magnetic field from 850 to 2000AD inferred from ^{10}Be records, *J. Geophys. Res.*, *109*, A12102, doi:10.1029/2004JA010633.

Clem, J. M., and L. I. Dorman (2000), Neutron monitor response functions, *Space Sci. Rev.*, *93*, 335–359.

Compton, A. H. (1934), Scientific work in the "Century of Progress" stratosphere balloon, *Proc. Natl. Acad. Sci.*, *20*, 79–81.

Compton, A. H., E. O. Wollan, and R. D. Bennett (1934), A precision recording cosmic-ray meter, *Rev. Sci. Ins.*, *5*, 415–422.

Damon, P. E., and C. P. Sonett (1991), Solar and terrestrial components of the atmospheric ^{14}C variation spectrum, in *The Sun in Time*, edited by C. P. Sonett, M. S. Giampapa, and M. S. Mathews, pp. 360–388, Univ. of Ariz. Press, Tucson, Ariz.

DeVorkin, D. H. (1989), *Race to the Stratosphere: Manned Scientific Ballooning in America*, Springer, New York.

Forbush, S. E. (1954), World-wide cosmic ray variations, 1937–1952, *J. Geophys. Res.*, *59*, 525–542.

Forbush, S. E. (1958), Cosmic ray intensity variations during two solar cycles, *J. Geophys. Res.*, *63*, 651–669.

Gleeson, L. J., and W. I. Axford (1968), Solar modulation of galactic cosmic rays, *Astrophys. J.*, *154*, 1011–1026.

Lal, D. (1987), ^{10}Be in polar ice: Data reflect changes in cosmic ray flux or polar meteorology, *Geophys. Res. Lett.*, *14*, 785–788.

Lange, I., and S. E. Forbush (1948), *Cosmic-Ray Results From Huancayo Observatory, Peru, June 1936–December, 1946*, *Res. of the Dept. of Terr. Magn.*, vol. XIV, Carnegie Inst. of Washington, Washington, D. C.

Lockwood, M., R. Stamper, and M. N. Wild (1999), A doubling of the Sun's coronal magnetic field during the past 100 years, *Nature*, *399*, 437–439.

McCracken, K. G. (2004), Geomagnetic and atmospheric effects upon the cosmogenic ^{10}Be observed in polar ice, *J. Geophys. Res.*, *109*, A04101, doi:10.1029/2003JA010060.

McCracken, K. G. (2007), Heliomagnetic field near Earth, 1428–2005, *J. Geophys. Res.*, *112*, A09106, doi:10.1029/2006JA012119.

McCracken, K. G., and B. Heikkila (2003), The cosmic ray intensity between 1933 and 1965, *Proc. Int. Conf. Cosmic Rays 28th*, 4117–4120.

McCracken, K. G., D. F. Smart, M. A. Shea, and G. A. M. Dreschhoff (2001a), 400 years of large fluence solar proton events, *Proc. Int. Conf. Cosmic Rays*, *27th*, 3209–3212.

McCracken, K. G., G. A. M. Dreschhoff, E. J. Zeller, D. F. Smart, and M. A. Shea (2001b), Solar cosmic ray events for the period 1561–1994: 1. Identification in the polar ice, 1561–1950, *J. Geophys. Res.*, *106*, 21,285–21,598.

McCracken, K. G., F. B. McDonald, J. Beer, G. Raisbeck, and F. Yiou (2004a), A phenomenological study of the long-term cosmic ray modulation, 850–1950 AD, *J. Geophys. Res.*, *109*, A12103, doi:10.1029/2004JA010685.

McCracken, K. G., G. A. M. Dreschhoff, D. F. Smart, and M. A. Shea (2004b), A study of the frequency of occurrence of large-fluence solar proton events and the strength of the interplanetary magnetic field, *Sol. Phys.*, *224*, 359–372.

Millikan, R. A., and G. H. Cameron (1928), New precision in cosmic ray measurements; yielding extensions of spectrum and indications of bands, *Phys. Rev.*, *31*, 921–930.

Mursula, K., I. G. Usoskin, and G. A. Kovaltsov (2003), Reconstructing the long-term cosmic ray intensity: Linear relations do not work, *Ann. Geophys.*, *21*, 863–867.

Muscheler, R., F. Joos, J. Beer, S. A. Muller, M. Vonmoos, and I. Snowball (2007), Solar activity during the past 1000 years inferred from radionuclide records, *Quat. Sci. Rev.*, *26*, 82–97.

Nagashima, K., S. Sakakibara, and K. Murakami (1989), Response and yield functions of neutron monitor, galactic cosmic-ray spectrum and its solar modulation, derived from all available world-wide surveys, *Nuovo Cimento*, *12*, 173–209.

Neher, H. V. (1953), An automatic ionization chamber, *Rev. Sci. Instrum.*, *24*, 99–102.

Neher, H. V. (1956), Low-energy primary cosmic-ray particles in 1954, *Phys. Rev.*, *103*, 228–236.

Neher, H. V. (1961), Cosmic-ray knee in 1958, *J. Geophys. Res.*, *66*, 4007–4012.

Neher, H. V. (1967), Cosmic ray particles that changed from 1954 to 1958 to 1965, *J. Geophys. Res.*, *72*, 1527–1539.

Neher, H. V. (1971), Cosmic rays at high latitudes and altitudes covering four solar maxima, *J. Geophys. Res.*, *76*, 1637–1651.

Neher, H. V., and H. R. Anderson (1964), Cosmic-ray intensity at Thule, Greenland, during 1962 and 1963 and a comparison with data from Mariner 2, *J. Geophys. Res.*, *69*, 807–814.

O'Brien, K. (1979), Secular variations in the production of the cosmogenic isotopes in the Earth's atmosphere, *J. Geophys. Res.*, *84*, 423–431.

Parker, E. N. (1958), Dynamics of the interplanetary gas and magnetic fields, *Astrophys. J.*, *128*, 664–676.

Parker, E. N. (1965), The passage of energetic particles through interplanetary space, *Planet. Space Sci.*, *13*, 9–13.

Peristykh, A. N., and P. E. Damon (2003), Persistence of the Gleissberg 88-year solar cycle over the past ~12,000 years: Evidence from cosmogenic isotopes, *J. Geophys. Res.*, *108*(A1), 1003, doi:10.1029/2002JA009390.

Rao, U. R. (1972), Solar modulation of galactic cosmic rays, *Space Sci Rev.*, *12*, 719–809.

Schrijver, C. J., M. L. DeRosa, and A. M. Tittle (2002), What is missing from our understanding of long-term solar and heliospheric activity?, *Astrophys. J.*, *577*, 1006–1012.

Shea, M. A., and D. F. Smart (2003), Preliminary study of the 400-year geomagnetic cutoff rigidity changes, cosmic rays and possible climate changes, *Proc. Int. Conf. Cosmic Rays 28th*, 4205–4208.

Solanki, S. K., M. Schussler, and M. Fligge (2000), Evolution of the Sun's large scale magnetic field since the Maunder minimum, *Nature*, *408*, 445–447.

Usoskin, I. G., and G. A. Kovaltsov (2006), Cosmic ray induced ionization in the atmosphere: Full modeling and practical applications, *J. Geophys. Res.*, *111*, D21206, doi:10.1029/2006JD007150.

Usoskin, I. G., G. K. Mursala, S. K. Solanki, M. Schussler, and G. A. Kovaltsov (2002), A physical reconstruction of cosmic ray intensity since 1610, *J. Geophys. Res.*, *107*(A11), 1374, doi:10.1029/2002JA009343.

Usoskin, I. G., S. K. Solanki, M. Schussler, K. Mursala, and K. Alanko (2003), Millennium-scale sunspot number reconstruction: Evidence for an unusually active sun since the 1940s, *Phys. Rev. Lett*, *91*, 211101.

Usoskin, I. G., S. K. Solanki, G. A. Kovaltsov, J. Beer, and B. Kromer (2006), Solar proton events in cosmogenic isotope data, *Geophys. Res. Lett.*, *33*, L08107, doi:10.1029/2006GL026059.

Wang, Y.-M., N. R. Sheeley, and J. Lean (2002), Role of a variable meridional flow in the secular evolution of the Sun's polar fields and open flux, *Astrophys. J.*, *577*, L53–L57.

Webber, W. R., and P. R. Higbie (2003), The production of cosmogenic Be nuclei in the Earth's atmosphere by cosmic rays: Its dependence on solar modulation and the interstellar cosmic ray spectrum, *J. Geophys. Res.*, *108*(A9), 1355, doi:10.1029/2003JA009863.

Webber, W. R., and J. A. Lockwood (2001), Voyager and Pioneer spacecraft measurements of cosmic ray intensities in the outer heliosphere: Towards a new paradigm for understanding the global modulation process: 1. Minimum solar modulation, *J. Geophys. Res.*, *106*, 29,323–29,331.

Webber, W. R., P. R. Higbie, and K. G. McCracken (2007), The production of the cosmogenic isotopes ^{3}H, ^{7}Be, ^{10}Be, ^{14}C, and ^{36}Cl in the Earth's atmosphere by solar and galactic cosmic rays, *J. Geophys. Res.*, doi:10.1029/2007JA012499, in press.

J. Beer, Swiss Federal Institute of Aquatic Science and Technology (EAWAG), CH-8600 Duebendorf, Switzerland.

K. G. McCracken, Institute for Physical Science and Technology, University of Maryland, 4247 CSS Building, College Park, MD 20742-2431, USA. (jellore@hinet.net.au)